Parametric Characterization of Neural Activity in the Locus Coeruleus in Response to Vagus Nerve Stimulation

Daniel R. Hulsey[1,2], **Jonathan R. Riley**[1,2], **Kristofer W. Loerwald**[2], **Robert L. Rennaker II**[1,2,3,*], **Michael P. Kilgard**[1,2], and **Seth A. Hays**[2,3,*]

[1]The University of Texas at Dallas, School of Behavioral Brain Sciences, BSB 14; Richardson, TX 75080

[2]Texas Biomedical Device Center, BSB 11, Richardson, TX 75080

[3]The University of Texas at Dallas, Erik Jonsson School of Engineering and Computer Science, 800 West Campbell Road, BSB 11, Richardson, TX 75080-3021

Abstract

Vagus nerve stimulation (VNS) has emerged as a therapy to treat a wide range of neurological disorders, including epilepsy, depression, stroke, and tinnitus. Activation of neurons in the locus coeruleus (LC) is believed to mediate many of the effects of VNS in the central nervous system. Despite the importance of the LC, there is a dearth of direct evidence characterizing neural activity in response to VNS. A detailed understanding of the brain activity evoked by VNS across a range of stimulation parameters may guide selection of stimulation regimens for therapeutic use. In this study, we recorded neural activity in the LC and the mesencephalic trigeminal nucleus (Me5) in response to VNS over a broad range of current amplitudes, pulse frequencies, train durations, inter-train intervals, and pulse widths. Brief 0.5 s trains of VNS drive rapid, phasic firing of LC neurons at 0.1 mA. Higher current intensities and longer pulse widths drive greater increases in LC firing rate. Varying the pulse frequency substantially affects the timing, but not the total amount, of phasic LC activity. VNS drives pulse-locked neural activity in the Me5 at current levels above 1.2 mA. These results provide insight into VNS-evoked phasic neural activity in multiple neural structures and may be useful in guiding the selection of VNS parameters to enhance clinical efficacy.

*Corresponding author information: The University of Texas at Dallas, Department of Bioengineering, 800 West Campbell Road, BSB11, Richardson, TX 75080-3021, seth.hays@utdallas.edu, Tel: 1-972-883-5236.

Introduction

More than 75,000 patients have received vagus nerve stimulation (VNS) therapy for the treatment of epilepsy and depression (Schlaepfer et al., 2008, Englot, Chang and Auguste., 2011, Berry et al., 2013, Ben-Menachem et al., 2015). Emerging studies provide evidence that VNS paired with rehabilitative training may be useful in the treatment of additional neurological disorders, including tinnitus and stroke (Dawson et al., 2016, De Ridder et al., 2014, Hays., 2016). Despite the widespread use of VNS, there is relatively little consensus on the optimal stimulation methods, perhaps owing to incomplete knowledge of the effects of VNS on structures throughout the brain. Therefore, a detailed understanding of the effects of VNS on neural activity in key structures may guide selection of stimulation parameters to maximize therapeutic benefits.

The noradrenergic locus coeruleus (LC) has been identified as a key mediator of VNS actions in the central nervous system. LC lesions block both the antiepileptic and antidepressant-like effects of VNS, demonstrating the requirement of noradrenergic engagement (Krahl et al., 1998, Grimonprez et al., 2015, Furmaga, Shah and Frazer., 2011). Moreover, 30 second trains of VNS increase firing rates of LC neurons over the course of minutes to hours (Groves, Bowman and Brown., 2005, Manta et al., 2009a, Manta et al., 2013, Dorr and Debonnel., 2006). Similar activation of brain structures, including the LC, is observed in human subjects minutes after delivery of VNS (Frangos, Ellrich and Komisaruk., 2015). Consistent with these actions on LC activity, VNS increases norepinephrine concentrations in the cortex and hippocampus on the order of minutes to hours (Hassert, Miyashita and Williams., 2004, Roosevelt et al., 2006, Follesa et al., 2007). Elevated norepinephrine is correlated with VNS-dependent seizure suppression, potentially linking LC activation to clinical efficacy (Raedt et al., 2011). Patients receiving VNS for epilepsy control demonstrate cumulative benefits after several months of stimulation (DeGiorgio et al., 2000, Ching et al., 2013), providing support for the notion that VNS promotes long-lasting changes to suppress seizures.

In addition to these protracted effects, there is accumulating evidence that VNS rapidly activates structures in the central nervous systems in milliseconds to seconds. The vagus nerve innervates the nucleus tractus solitarius, which sends excitatory input to the LC via the nucleus paragigantocellularis, providing a pathway by which VNS could directly drive short latency spiking in the LC (Ruffoli et al., 2011). Indirect evidence from measures of cortical excitability suggests that VNS-dependent activation of neuromodulatory circuits rapidly influences cortical activity. Within 10 milliseconds of stimulation, VNS triggers scalp-recorded evoked potentials, reflecting ascending neural activation (Usami et al., 2013). Moreover, VNS modulates cortical synchrony via activation of the cholinergic system within 100 milliseconds of stimulation (Nichols et al., 2011). A recent study indicates that this

rapid activation is required for VNS-dependent enhancement of plasticity (Engineer et al., 2011). Delivery of 0.5 s trains of VNS coincident with tones drives robust plasticity in auditory cortex that is specific to frequency of the paired tone. However, equivalent VNS delivered 15 s before or after tones fails to drive plasticity, indicating that VNS engenders rapid, phasic neural activation to support plasticity. Despite its potential importance in the functional consequences of VNS, little is known about the rapid action of VNS on neural activity in relevant brain structures. A detailed understanding of the rapid modulation of activity may lead to the development of optimized stimulation protocols that capitalize on these temporal patterns.

A clear understanding of stimulation intensity-dependent modulation of activity is also critical to maximizing the effects of VNS. Studies evaluating the memory- and plasticity-enhancing effects of VNS across a range of stimulation parameters report an inverted-U response, in which moderate intensity stimulation yields a greater effect than lower or higher intensities (Clark et al., 1998, Clark et al., 1999, Borland et al., 2016). One plausible explanation for the inverted-U response is VNS-dependent activation of a low threshold system that promotes plasticity and an overriding high threshold system that occludes plasticity. The majority of parameter optimization efforts have focused on driving greater activity in target structures, including the LC (Manta et al., 2009b). This has proven informative in the context of seizure suppression, in which stronger VNS paradigms appear to yield greater suppression (Ghani et al., 2015). However, the complex inverted-U effect of VNS on plasticity suggests that minimization of off-target responses may be equally useful and necessary to maximize therapeutic effects.

Materials and Methods

Subjects

The University of Texas at Dallas Institutional Animal Care and Use Committee approved all procedures. Female Sprague Dawley rats (Charles River), weighing $310 \pm 11g$, were used in all experiments. Rats were housed in a 12:12 hr reversed light cycle environment with ad libitum access to food and water.

Surgical Procedures

Rats were anesthetized with ketamine hydrochloride (80 mg/kg, i.p.) and xylazine (10 mg/kg, i.p.). Supplemental doses were administered as needed to maintain anesthesia throughout surgical procedures and data collection. Carprofen (5mg/kg, s.c.) was administered to reduce inflammation. Body temperature was maintained throughout surgery and neural recording using a feedback-controlled electric warming pad (FHC, Bowdoin, ME). Subjects were implanted with a custom made platinum-iridium bipolar stimulating cuff electrode on the left cervical vagus nerve, as previously described (Engineer et al., 2011, Khodaparast et al., 2013, Khodaparast et al., 2014, Hays et al., 2014, Pruitt et al., 2016, Khodaparast et al., 2016, Hays et al., 2016, Hulsey et al., 2016). A transient drop in blood oxygen saturation in response to a short (~3 sec) VNS train was used to confirm that the cuff electrode was functional. Immediately after cuff implantation, subjects were positioned in a stereotaxic frame with bregma and lambda level. After exposing the surface of the skull, a

hole was drilled centered at 1.1mm lateral and 3.6mm caudal to lambda and the underlying dura was carefully removed (George et al., 2013).

Electrophysiological Recordings in LC and Me5

Extracellular recording was performed with parylene coated tungsten microelectrodes (2–4 MΩ, FHC). Two electrodes (250 μm spacing) were lowered approximately 5.5–6.5 mm ventral from the dural surface at a 15 degree angle from the vertical axis until neural activity with appropriate response characteristics (described below) was observed. Neural signals were differentially amplified using an RA16PA preamplifier (Tucker-Davis Technologies, Alachua, FL) from a common reference and ground attached to the skin around the skull. Signals were digitized at 24.414 ks/s with 16-bit resolution using an RZ5 BioAmp processor (Tucker-Davis Technologies) and monitored online with Brainware. LC units were identified by a characteristic response to a hindpaw pinch of a phasic burst of spikes followed by inhibition, long duration positive-negative waveforms with a notch on the ascending phase, and spontaneous firing rate (Martins and Froemke., 2015) (Fig. 1). The Me5 nucleus is located lateral to the LC and was identified by high frequency firing, accompanied by burst firing upon manipulation of the jaw (Linden., 1978) (Fig. 6A). Multi-unit recordings were made at sites identified as LC or Me5. Electrophysiological recording sweeps were 4.5 s in duration, and were initiated every 8 s (except as noted). One second of spontaneous activity was recorded prior to VNS presentation. A subset of recording sites contained readily identifiable single units. After complete stimulus set presentation at a site, the electrodes were advanced at least 100 μm and a new recording site was identified. In a subset of animals, electrolytic lesions were made at the final recording location to confirm electrode position (Fig 1D).

Vagus Nerve Stimulation

VNS was delivered through a constant current stimulus isolation unit (Model 2200, A-M Systems). The vagus nerve was stimulated at standard parameters of sixteen 0.8 mA 100 μs biphasic pulses at 30 Hz (Engineer et al., 2011, Porter et al., 2011, Borland et al., 2016, Hulsey et al., 2016). In addition, a broad stimulus set was delivered with varying pulse number per train (0 – 64 pulses), stimulation current intensity (0 – 2.5 mA), pulse frequency (0 – 120 Hz), and pulse width (0 – 500 μs) totaling 23 distinct stimulation parameters (Tables 1–3). Every VNS parameter was presented 20 times in a pseudorandom, interleaved order at each recording site. The main recording protocol lasted approximately 40 minutes at each site. At a subset of sites, standard parameter stimulation was delivered with 5 and 30 second inter-train intervals. Cuff voltage was monitored throughout data collection procedures.

Data Analysis and Statistical Methods

Data was processed using custom MATLAB software (MathWorks). Electrical stimulation artifact was removed from data by linearly interpolating between data points 0.2 ms before and 3 ms after each pulse in a VNS train. The neural signal was bi-directionally band pass filtered between 300–3000Hz. Spike activity for multiunit responses were automatically detected by positive crossings of a threshold initially set at 2.58 times greater than the standard deviation (99 percent confidence interval) of the signal for the entire stimulus set

and adjusted as necessary to distinguish spiking activity. Spike data was sorted by VNS parameter and a mean peristimulus time histogram (PSTH) was generated with 50 ms bins. Firing rate in Hz was calculated by summing all spikes per 50 ms bin and dividing by bin time in seconds. Phasic excitatory responses were calculated as driven spikes (sum of spikes at a given parameter – sum spontaneous spikes) from 1–750 ms after stimulation onset for all 500 ms VNS trains. An offset response was calculated from 751–1500ms as percent change from the spontaneous rate. For experiments evaluating the effects of varying VNS frequency, driven spikes were calculated based on positive response periods for each stimulus. Spike data during stimulation artifact cutout was interpolated to normalize cutout duration across frequencies. A cycle histogram of spiking activity after each pulse was created and vector strength calculations were used to quantify the degree of synchronization between VNS pulse timing and neural spiking activity (Shetake et al., 2011). For vector strength analysis, a value of 1 indicates perfect synchronization and 0 indicates no synchronization to VNS pulses. Repeated measures analysis of variance (ANOVA) followed by paired t-tests (Bonferroni corrected to an alpha of 0.007) were used where appropriate to determine significant differences.

Histology

Upon completion of daily recording, an electrolytic lesion was made by delivering current through one of the electrodes at the final recording site (1 mA current, 30 s). Immediately after electrolytic lesion, animals were transcardially perfused with phosphate buffered saline followed by 4% paraformaldehyde in phosphate-buffered saline (PBS). Brains were post-fixed for at least 24 hours and transferred to 20% sucrose solution for cryoprotection. The extent of the LC was sectioned with 40 μm sections. Sections were stained for tyrosine hydroxylase (TH) to identify the LC. In brief, sections were incubated in a permeabilization buffer of 0.3% triton in PBS, followed by a quenching solution of 0.3% H_2O_2 in methanol. After washing in PBS, sections were incubated in a blocking solution of 5% normal horse serum at room temperature for 1 hour. Tissue was then transferred to primary TH antibody (Cat # AB152, EMD Millipore) at a 1:1000 dilution and incubated overnight at 4°C. The following day, sections were processed with horseradish peroxidase substrate (Vectastain ABC Elite, Vectorlabs) and stained with diaminobenzidine (ImmPACT DAB, Vectorlabs). Sections were then mounted on microscope slides dried, and cover slipped using DPX mounting medium (Cat #13512, EMS). TH staining and lesions were visualized using an Olympus BX51 microscope and imaged at 4x magnification using an Olympus DP71 acquisition system.

Results

VNS drives activity in LC neurons

LC neurons were identified according to stereotaxic location and well-validated electrophysiological characteristics: wide spike widths and consistent excitation-inhibition pattern in response to a hindpaw pinch (Martins and Froemke., 2015) (Fig. 1A & C). Electrode placement was histologically verified in a subset of animals (Fig. 1D). Electrophysiological recordings were made from 23 sites across 5 animals. A 0.5 s train of 0.8 mA, 100 μs biphasic pulses delivered at 30 Hz reliably evoked rapid, robust phasic

neural activity in the LC (Fig. 1B & 2). Peak firing rate of the phasic response was increased approximately 450% over spontaneous firing rate. All LC recording sites (23 of 23) demonstrated significant increases in firing rate with these stimulation parameters. Longer train durations resulted in a linear increase in driven spikes (Table 1; Fig. 2C; Repeated measures ANOVA, $F[3,66] = 74.22$, $p < 0.0001$; 4 pulses: 14.5 ± 1.9 spikes, 16 pulses: 41.3 ± 4.2 spikes, 64 pulses: 131.2 ± 15.0 spikes, paired t-tests vs. spontaneous, all $p < 0.0001$). Similar increases in firing rate were observed for 5 and 30 second inter-train intervals (5 s ITI: 53.2 ± 5.8, 30 s ITI: 54.6 ± 9.4; Paired t-test, $p = 0.69$). These findings indicate that short trains of VNS drive rapid, phasic neural activity in the LC.

Effects of stimulation intensity on LC neural activity

Stimulation intensity influences VNS-dependent norepinephrine release, neural plasticity, memory enhancement, and clinical seizure suppression, suggesting that neural activity in the LC activity is modulated by VNS intensity (Clark et al., 1995, Clark et al., 1999, Roosevelt et al., 2006, Zuo, Smith and Jensen., 2007a, Ghani et al., 2015, Borland et al., 2016). We examined LC firing rate across a range of VNS stimulation intensities from 0.1 to 2.5 mA, while holding other parameters constant (Fig 3A; Table 2). Firing rate was slightly, but significantly, increased at a stimulation intensity of 0.1 mA, consistent with recruitment of A and B fibers (Groves and Brown., 2005) (Fig. 3C&D; 0 mA: 13.7 ± 1.3; 0.1 mA: 20.8 ± 2.1; Paired t-test v. spontaneous, $p < 0.0001$). Driven activity increased monotonically across the range of stimulation intensities and was significantly increased at each tested intensity above 0.1 mA (Fig. 3D&E; Repeated measures ANOVA, $F[7,154] = 126.44$, $p < 0.0001$; Paired t-tests, 0 mA v. 0.2 – 2.5mA, all $p < 0.001$). Increasing stimulation intensity resulted in a shorter latency to the onset of significantly driven activity (Fig 3E). Well-isolated single units in a subset of electrophysiological recordings exhibited a similar monotonically increasing firing rate in response to greater stimulation intensities (Fig. 3A&B; Repeated measures ANOVA, $F[7,133] = 30.29$, $p < 0.0001$; Paired t-tests, 0 mA v. 0.4 – 2.5mA, all $p < 0.001$). An offset response (751 – 1500 ms) was observed that displayed a modest, non-monotonic change in firing rate with increasing current (Fig. 3E inset). Stimulation intensities from 0.2 – 0.8 mA resulted in a 20% suppression of neural activity compared to spontaneous rate during the offset response, while stimulation intensities at 1.6 mA and 2.5 mA demonstrated a 30% increase in firing rate (Fig. 3F). These findings indicate LC neurons are engaged by VNS at low thresholds and that increasing stimulation intensities drive greater phasic neural activity.

Effects of pulse frequency on LC neural activity

We next sought to determine the effect of varying the frequency of pulses within a stimulation train on neural activity in the LC. Stimulation frequency was varied from 7.5 Hz to 120 Hz, while all other parameters, including number of pulses per train, were held constant (Fig. 4; Table 3). Firing rate was significantly increased at all frequencies tested (Fig. 4C; Repeated measures ANOVA, $F[5,110] = 73.47$, $p < 0.0001$; Paired t-tests, 0 Hz v. 7.5 – 120 Hz, all $p < 0.001$). The temporal profile of LC activity reveals that higher stimulation frequencies result in greater maximal discharge rates over a shorter duration (Fig. 4B). However, the total number of driven spikes in response to a VNS train was similar at most frequencies (Fig. 4C). A slight, but significant reduction in total driven spikes was

observed at 120 Hz compared to 30 Hz (Paired t-test, 30 Hz v. 120 Hz, p < 0.0001). These results suggest that, for a fixed number of pulses, varying VNS frequency affects the timing, but not total amount of LC activity.

Effects of pulse width on LC neural activity

Pulse width influences tolerability and efficacy of VNS therapy; therefore, identification of parameters that maximize LC activity at minimal pulse widths may guide selection of clinical parameters (Liporace et al., 2001, Heck, Helmers and DeGiorgio., 2002). Pulse width was varied from 30 μs to 500 μs at various current intensities while all other parameters were held constant (Table 4). At a stimulation intensity of 0.8 mA, pulse widths of 30 μs and greater resulted in significantly driven, monotonically increasing neural activity (Fig. 5A; Repeated measures ANOVA, F[3,66] = 155.57, p < 0.0001; Paired t-tests, 0 μs v. 30 – 500 μs, all p < 0.0001). Similarly, longer pulse widths drove significantly greater firing rates at all current intensities tested (Fig. 5A; Repeated measures ANOVA, 0.2 mA: F[2,44] = 96.23, p < 0.0001; Paired t-tests, 0 μs v. 100, 500 μs, all p < 0.0001; 0.4 mA: F[2, 44] = 154.36, p < 0.0001; Paired t-tests, 0 μs v. 100, 500 μs, all p < 0.0001; 1.6 mA: F[3,66] = 107.78, p < 0.0001; Paired t-tests, 0 μs v. 30, 60, and 100 μs, all p < 0.0001). Evaluation of driven activity as a function of total charge per pulse (pulse width × current intensity) allowed direct comparison of parameter sets with different pulse widths and intensities. Independent of current intensity and pulse width, LC activity increases approximately linearly up to an apparent plateau around 160 nC per pulse, after which greater charge delivery does not yield significantly increased LC activity (Fig. 5B; 160 nC vs. 400 nC; Paired t-test, p = 0.24).

Neural activity in the mesencephalic trigeminal nucleus (Me5) in response to varying VNS parameters

There is growing evidence that the beneficial effects of VNS are limited to moderate current levels (Clark et al., 1995, Clark et al., 1998, Clark et al., 1999, Zuo, Smith and Jensen., 2007b, Borland et al., 2016). It has been proposed that higher current levels may activate responses in other brain regions that limit the effective range of VNS. To test this hypothesis, we compared VNS-dependent activity in the LC to activity in the neighboring mesencephalic trigeminal nucleus (Me5). Me5 receives diverse sensory and proprioceptive input from many locations, including jaw musculature (Alvarado-Mallart et al., 1975, Jerge., 1963). We recorded multiunit neural activity in 26 sites in Me5 across 8 animals. Me5 neurons were identified by a strong response to changes in jaw position, as previously reported (Linden., 1978) (Fig. 6A). VNS resulted in short latency driven activity in Me5 neurons after each individual pulse within a stimulation train, distinct from that observed in the LC (Fig. 6B&C). Vector strength at 1.6 mA was significantly stronger in the Me5 compared to LC, highlighting the pulse-locked activity pattern in Me5 neurons (Me5: 0.47 ± .04, LC: 0.13 ± .01; Unpaired t-test, p < 0.001). The threshold to drive neural activity was substantially higher than that observed for the LC, with only stimulation intensities at or above 1.2 mA yielding significant driven activity in Me5 neurons (Fig. 6D; One-Way ANOVA, F[7,84] = 35.13, p < 0.0001; Paired t-tests compared to 0 mA, p < 0.0001 for 1.2, 1.6, and 2.5 mA). Analysis of vector strength and threshold current intensity needed to evoke significantly driven activity illustrates the distinct VNS response characteristics

observed in Me5 and LC neurons (Fig. 7). These findings demonstrate that Me5 neurons exhibit monotonic increases in phase-locked firing rate in response to VNS at stronger stimulation intensities than LC neurons.

Discussion

In this study, we assessed the response of LC neurons across a range of commonly used VNS parameters. Brief bursts of VNS drive rapid, phasic neural activity in the LC. Significantly driven phasic responses are observed at low (0.1 mA) stimulation intensities. Increasing the current intensity and pulse width drives greater neural activity. Varying the frequency of a fixed number of pulses affects the timing, but not the total amount of LC activity. The mesencephalic trigeminal nucleus, a brainstem nucleus nearby the LC that receives sensory input from laryngeal muscles, exhibits distinct pulse-locked neural activity in response to stronger stimulation intensities. Together, these findings provide insight into the neural responses to VNS in multiple brain regions and may be useful in selecting parameters to optimize VNS for clinical applications.

The ability of VNS to modulate neural activity in the LC corroborates previous studies which have examined this relationship over longer time scales (Groves, Bowman and Brown., 2005, Dorr and Debonnel., 2006). Here, we extend these findings and show that short bursts of VNS evoke rapid, phasic neural activity in the LC. This rapid recruitment of LC neurons likely mediates the memory- and plasticity-enhancing effects of VNS. We speculate that the short latency increase in LC activity drives a phasic release of norepinephrine which acts to facilitate plasticity specific to ongoing experience (Hays., 2016). The role of the LC in plasticity is supported by evidence that antagonism of β-adrenergic receptors blocks VNS-dependent plasticity (Shen et al., 2012). Moreover, enhanced plasticity requires coincident (or closely-timed) presentation of VNS with stimuli, highlighting the importance of rapid activation of brain structures in the functional consequences of VNS (Engineer et al., 2011). Longer trains of VNS also facilitate plasticity, but considering the efficacy of short trains of VNS, it is likely that the initial rapid increase in firing rate mediates the majority of the effect (Zuo, Smith and Jensen., 2007b).

Stimulation intensities at 0.1 mA were sufficient to drive neural activity in the LC, suggesting that phasic activity is regulated, at least in part, by A- and B-fiber activation. Vagal C-fibers would not be expected to be activated at this low intensity (Woodbury and Woodbury., 1990). However, the increasing magnitude of LC activation suggests that C-fibers may also contribute at higher stimulation intensities. Given the role of norepinephrine levels in the reduction of seizures (Raedt et al., 2011), activation of the LC with low intensity stimulation supports the notion that C-fiber activation is unnecessary for the seizure suppressing effects of VNS (Krahl, Senanayake and Handforth., 2001). A notable limitation of the present study is the use of an anesthetized recording preparation. Application of α2-agonists for anesthesia, including xylazine used in combination with ketamine in this study, reduces spontaneous neural activity in the LC (Aghajanian and VanderMaelen., 1982, Aston-Jones et al., 1994, Berridge and Waterhouse., 2003). While excitability is reduced, the large magnitude of VNS-driven responses observed in LC neurons in this study suggests that similar, if not larger, increases in activity would be observed in the absence of anesthesia.

Future efforts should examine VNS-dependent LC dynamics across a range of parameters in unanesthetized conditions.

Both greater current intensities and longer pulse widths increase firing rate in the LC. These findings are consistent with previous studies that indicate that stronger stimulation intensities yield greater increases in norepinephrine levels in cortical structures (Roosevelt et al., 2006). Improved seizure suppression is associated with higher levels of VNS-induced norepinephrine levels in an animal model of epilepsy, suggesting that greater LC activation may mediate the anti-epileptic effects of VNS (Raedt et al., 2011). Indeed, a meta-analysis examining the effect of VNS intensity on seizure suppression revealed that stronger stimulation parameters correlate with better clinical efficacy (Ghani et al., 2015). Increased activity in the LC in response to stronger VNS intensities likely represents the mechanistic link between increased stimulation current and better seizure suppression.

There is a dearth of direct evidence to define the optimal stimulation frequency for VNS. Our findings indicate that the timing, but not the total amount, of neural activity in the LC is influenced by frequency for a fixed number of pulses over the range tested. Higher frequencies elicit greater increases in LC firing rate over a shorter period of time. This modulation of spike rate over time by varying pulse frequency and train duration would, in principle, allow control of the temporal profile of norepinephrine levels. For instance, a short, high frequency train may drive a strong, transient release of norepinephrine, while a long, low frequency train would yield a smaller, more sustained increase in norepinephrine. These findings provide a rationale for more detailed investigation into the functional consequences of different stimulation frequencies.

Charge delivery influences tolerability of VNS in patients (Liporace et al., 2001, Heck, Helmers and DeGiorgio., 2002). Reductions in current intensity and pulse width reduce charge delivery and can be used to modify tolerability of the therapy and provide longer implantable pulse generator battery life. However, higher current intensities and longer pulse widths increase charge delivery and are associated with greater clinical efficacy, pointing to a trade-off between minimizing side-effects and maximizing therapeutic benefit (Ghani et al., 2015, Heck, Helmers and DeGiorgio., 2002). The characterization of LC activation as a function of charge delivery in this study indicates that charge increases firing rate up to an apparent plateau at approximately 160 nC, after which additional charge yields substantially diminishing gains in LC activity. Additional studies are needed to fully characterize this relationship across a wider range of parameters, including potential interaction with train duration and pulse frequency.

In addition to the LC, the mesencephalic trigeminal nucleus exhibits driven neural activity in response to VNS. The pattern of activation in Me5 neurons is distinct from that observed in the LC, displaying strongly pulse-locked activation to each pulse within a VNS train. The Me5 receives sensory and proprioceptive input from external laryngeal muscles, including the digastricus and mylohyoideus (Alvarado-Mallart et al., 1975). VNS is known to drive activation of laryngeal muscles (Castoro et al., 2011). While we cannot make a direct assertion with the data from this study, we speculate that the phase-locked neural activity in Me5 reflects activation of proprioceptive neurons as a result of VNS-dependent contraction

of laryngeal musculature. Increasing VNS current intensity drives greater EMG responses, consistent with the increased Me5 activity reported in our study (Castoro et al., 2011). The observation of VNS-driven activity in Me5 provides an intriguing link to voice alterations common in patients receiving VNS, as the same laryngeal muscles associated with speech production send proprioceptive input to the Me5 (Sokolowsky., 1943, Sataloff, Heman-Ackah and Hawkshaw., 2007, DeGiorgio et al., 2000). Because the threshold stimulation current that yields activation in Me5 was substantially higher (1.2 mA) than that required to drive activity in the LC (0.1 mA), it may be possible to identify stimulation parameter sets that minimize Me5 activation to reduce adverse effects on voice while maintaining therapeutic efficacy.

Targeted plasticity therapies using short bursts of VNS paired with rehabilitative training regimens have emerged as potential treatments for a variety of neurological disorders (Hays., 2016). Preclinical studies demonstrate that VNS paired with rehabilitative training improves recovery in models of tinnitus, ischemic and hemorrhagic stroke, and traumatic brain injury (Engineer et al., 2011, Khodaparast et al., 2013, Khodaparast et al., 2014, Hays et al., 2014, Pruitt et al., 2016, Khodaparast et al., 2016, Hays et al., 2016). Moreover, clinical studies provide an initial indication of the clinical utility of VNS-based plasticity therapies for tinnitus and stroke patients (Dawson et al., 2016, De Ridder et al., 2014). Because of its clear link to plasticity and engagement by VNS, the LC represents a likely mediator of VNS-dependent enhancement of plasticity. Other neuromodulatory systems likely act synergistically to contribute, but VNS-driven phasic activation of LC reported here provide evidence that noradrenergic circuitry is activated at VNS parameters that effectively enhance plasticity (Seol et al., 2007, Shetake et al., 2011, Porter et al., 2011, He et al., 2015, Engineer et al., 2015, Hulsey et al., 2016).

Several studies evaluating the memory- and plasticity-enhancing effects of VNS have reported an inverted-U response, in which middle intensity stimulation yields greater effects than low or high stimulation intensities (Clark et al., 1995, Clark et al., 1999, Zuo, Smith and Jensen., 2007a, Borland et al., 2016). Given the potential role for the LC in VNS-dependent enhancement of plasticity, it was possible that neural activity in the LC would exhibit a similar inverted-U relationship, in which moderate stimulation intensities elicit maximal driven spikes. However, the observed monotonically increasing phasic excitation of the LC with stimulation intensity does not support this conclusion, suggesting that firing rate in the LC itself does not mediate the inverted-U response. However, it is possible that presynaptic depletion or noradrenergic autoinhibition at strong stimulation intensities may limit norepinephrine release without directly suppressing neural activity in LC (Starke., 1981). Interestingly, the offset response to VNS (from 751 to 1500 ms) fits empirical data of the plasticity-enhancing effects of VNS (Borland et al., 2016). Many explanations could account for the inverted-U response. One likely model is a low-threshold system that drives positive effects and an overriding high-threshold system that drives negative effects (Hays., 2016). It is tempting to relate the LC as the positive system and Me5 as the negative system. Such a model would closely fit the experimental evidence of the inverted-U effect of VNS on plasticity, as stimulation parameters that drive maximal LC activity in the absence of Me5 activity (0.8 mA) yields the greatest enhancement of cortical plasticity (Borland et al., 2016). However, this model is unlikely to be complete, because while the pro-plasticity role

of the LC is easily recognized, there is no clear evidence that would establish Me5 as the negative system to suppress the positive effects of the LC. However, it is conceivable that a different, yet-to-be-identified system with activation characteristics similar to that of the Me5 could interact with LC activation to account for the inverted-U response. Defining the inverted-U is of considerable clinical importance for VNS-based plasticity therapies, as more stimulation does not necessarily relate to greater efficacy.

Acknowledgments

References

Aghajanian GK, VanderMaelen CP. Alpha 2-Adrenoceptor-Mediated Hyperpolarization of Locus Coeruleus Neurons: Intracellular Studies in Vivo. Science. 1982; 215:1394–1396. [PubMed: 6278591]

Alvarado-Mallart M, Batini C, Buisseret-Delmas C, Corvisier J. Trigeminal representations of the masticatory and extraocular proprioceptors as revealed by horseradish peroxidase retrograde transport. Experimental brain research. 1975; 23:167–179. [PubMed: 1081052]

Aston-Jones G, Rajkowski J, Kubiak P, Alexinsky T. Locus coeruleus neurons in monkey are selectively activated by attended cues in a vigilance task. J Neurosci. 1994; 14:4467–4480. [PubMed: 8027789]

Ben-Menachem E, Revesz D, Simon B, Silberstein S. Surgically implanted and non-invasive vagus nerve stimulation: a review of efficacy, safety and tolerability. European Journal of Neurology. 2015; 22:1260–1268. [PubMed: 25614179]

Berridge CW, Waterhouse BD. The locus coeruleus–noradrenergic system: modulation of behavioral state and state-dependent cognitive processes. Brain Res Rev. 2003; 42:33–84. [PubMed: 12668290]

Berry SM, Broglio K, Bunker M, Jayewardene A, Olin B, Rush AJ. A patient-level meta-analysis of studies evaluating vagus nerve stimulation therapy for treatment-resistant depression. Med Devices (Auckl). 2013; 6:17–35. [PubMed: 23482508]

Borland MS, Vrana WA, Moreno NA, Fogarty EA, Buell EP, Sharma P, Engineer CT, Kilgard MP. Cortical Map Plasticity as a Function of Vagus Nerve Stimulation Intensity. Brain Stimulation. 2016; 9:117–123. [PubMed: 26460200]

Castoro MA, Yoo PB, Hincapie JG, Hamann JJ, Ruble SB, Wolf PD, Grill WM. Excitation properties of the right cervical vagus nerve in adult dogs. Exp Neurol. 2011; 227:62–68. [PubMed: 20851118]

Ching J, Khan S, White P, Reed J, Ramnarine D, Sieradzan K, Sandeman D. Long-term effectiveness and tolerability of vagal nerve stimulation in adults with intractable epilepsy: a retrospective analysis of 100 patients. Br J Neurosurg. 2013; 27:228–234. [PubMed: 23113878]

Clark K, Krahl S, Smith D, Jensen R. Post-training unilateral vagal stimulation enhances retention performance in the rat. Neurobiol Learn Mem. 1995; 63:213–216. [PubMed: 7670833]

Clark K, Smith D, Hassert D, Browning R, Naritoku D, Jensen R. Posttraining electrical stimulation of vagal afferents with concomitant vagal efferent inactivation enhances memory storage processes in the rat. Neurobiol Learn Mem. 1998; 70:364–373. [PubMed: 9774527]

Clark KB, Naritoku DK, Smith DC, Browning RA, Jensen RA. Enhanced recognition memory following vagus nerve stimulation in human subjects. Nat Neurosci. 1999; 2:94–98. [PubMed: 10195186]

Dawson J, Pierce D, Dixit A, Kimberley TJ, Robertson M, Tarver B, Hilmi O, McLean J, Forbes K, Kilgard MP, Rennaker RL, Cramer SC, Walters M, Engineer N. Safety, Feasibility, and Efficacy of Vagus Nerve Stimulation Paired with Upper-Limb Rehabilitation after Ischemic Stroke. Stroke. 2016; 47:143–150. [PubMed: 26645257]

De Ridder D, Vanneste S, Engineer ND, Kilgard MP. Safety and Efficacy of Vagus Nerve Stimulation Paired with Tones for the Treatment of Tinnitus: A Case Series. Neuromodulation: Technology at the Neural Interface. 2014; 17(2):170–9.

DeGiorgio C, Schachter S, Handforth A, Salinsky M, Thompson J, Uthman B, Reed R, Collin S, Tecoma E, Morris G. Prospective long-term study of vagus nerve stimulation for the treatment of refractory seizures. Epilepsia. 2000; 41:1195–1200. [PubMed: 10999559]

Dorr AE, Debonnel G. Effect of vagus nerve stimulation on serotonergic and noradrenergic transmission. J Pharmacol Exp Ther. 2006; 318:890–898. [PubMed: 16690723]

Engineer CT, Engineer ND, Riley JR, Seale JD, Kilgard MP. Pairing Speech Sounds With Vagus Nerve Stimulation Drives Stimulus-specific Cortical Plasticity. Brain Stimulation. 2015; 8(3):637–44. [PubMed: 25732785]

Engineer ND, Riley JR, Seale JD, Vrana WA, Shetake JA, Sudanagunta SP, Borland MS, Kilgard MP. Reversing pathological neural activity using targeted plasticity. Nature. 2011; 470:101–104. [PubMed: 21228773]

Englot DJ, Chang EF, Auguste KI. Vagus nerve stimulation for epilepsy: a meta-analysis of efficacy and predictors of response: A review. J Neurosurg. 2011; 115:1248–1255. [PubMed: 21838505]

Follesa P, Biggio F, Gorini G, Caria S, Talani G, Dazzi L, Puligheddu M, Marrosu F, Biggio G. Vagus nerve stimulation increases norepinephrine concentration and the gene expression of BDNF and bFGF in the rat brain. Brain Res. 2007; 1179:28–34. [PubMed: 17920573]

Frangos E, Ellrich J, Komisaruk BR. Non-invasive access to the vagus nerve central projections via electrical stimulation of the external ear: fMRI evidence in humans. Brain stimulation. 2015; 8:624–636. [PubMed: 25573069]

Furmaga H, Shah A, Frazer A. Serotonergic and noradrenergic pathways are required for the anxiolytic-like and antidepressant-like behavioral effects of repeated vagal nerve stimulation in rats. Biol Psychiatry. 2011; 70:937–945. [PubMed: 21907323]

George SA, Knox D, Curtis AL, Aldridge JW, Valentino RJ, Liberzon I. Altered locus coeruleus–norepinephrine function following single prolonged stress. Eur J Neurosci. 2013; 37:901–909. [PubMed: 23279008]

Ghani S, Vilensky J, Turner B, Tubbs R, Loukas M. Meta-analysis of vagus nerve stimulation treatment for epilepsy: correlation between device setting parameters and acute response. Child's Nervous System. 2015; 31:2291–2304.

Grimonprez A, Raedt R, Portelli J, Dauwe I, Larsen LE, Bouckaert C, Delbeke J, Carrette E, Meurs A, De Herdt V. The antidepressant-like effect of vagus nerve stimulation is mediated through the locus coeruleus. J Psychiatr Res. 2015; 68:1–7. [PubMed: 26228393]

Groves DA, Brown VJ. Vagal nerve stimulation: a review of its applications and potential mechanisms that mediate its clinical effects. Neuroscience & Biobehavioral Reviews. 2005; 29:493–500. [PubMed: 15820552]

Groves DA, Bowman EM, Brown VJ. Recordings from the rat locus coeruleus during acute vagal nerve stimulation in the anaesthetised rat. Neurosci Lett. 2005; 379:174–179. [PubMed: 15843058]

Hassert D, Miyashita T, Williams C. The effects of peripheral vagal nerve stimulation at a memory-modulating intensity on norepinephrine output in the basolateral amygdala. Behav Neurosci. 2004; 118:79. [PubMed: 14979784]

Hays SA. Enhancing Rehabilitative Therapies with Vagus Nerve Stimulation. Neurotherapeutics. 2016; 13(2):382–94. [PubMed: 26671658]

Hays SA, Ruiz A, Bethea T, Khodaparast N, Carmel JB, Rennaker RL, Kilgard MP. Vagus nerve stimulation during rehabilitative training enhances recovery of forelimb function after ischemic stroke in aged rats. Neurobiol Aging. 2016; 43:111–118. [PubMed: 27255820]

Hays SA, Khodaparast N, Hulsey DR, Ruiz A, Sloan AM, Rennaker RL II, Kilgard MP. Vagus Nerve Stimulation during Rehabilitative Training Improves Functional Recovery after Intracerebral Hemorrhage. Stroke. 2014; 45:10–3097. [PubMed: 24203850]

He K, Huertas M, Hong S, Tie X, Hell J, Shouval H, Kirkwood A. Distinct Eligibility Traces for LTP and LTD in Cortical Synapses. Neuron. 2015; 88:528–538. [PubMed: 26593091]

Heck C, Helmers SL, DeGiorgio CM. Vagus nerve stimulation therapy, epilepsy, and device parameters Scientific basis and recommendations for use. Neurology. 2002; 59:S31–S37. [PubMed: 12270966]

Hulsey DR, Hays SA, Khodaparast N, Ruiz A, Das P, Rennaker RL, Kilgard MP. Reorganization of Motor Cortex by Vagus Nerve Stimulation Requires Cholinergic Innervation. Brain Stimulation. 2016; 9(2):174–81. [PubMed: 26822960]

Jerge C. Organization and function of the trigeminal mensencephalic nucleus. J Neurophysiol. 1963; 26:379–392. [PubMed: 13957676]

Khodaparast N, Hays SA, Sloan AM, Fayyaz T, Hulsey DR, Rennaker RL II, Kilgard MP. Vagus nerve stimulation delivered during motor rehabilitation improves recovery in a rat model of stroke. Neurorehabil Neural Repair. 2014; 28:698–706. [PubMed: 24553102]

Khodaparast N, Kilgard MP, Casavant R, Ruiz A, Qureshi I, Ganzer PD, Rennaker RL 2nd, Hays SA. Vagus Nerve Stimulation During Rehabilitative Training Improves Forelimb Recovery After Chronic Ischemic Stroke in Rats. Neurorehabil Neural Repair. 2016; 30(7):676–684. [PubMed: 26542082]

Khodaparast N, Hays SA, Sloan AM, Hulsey DR, Ruiz A, Pantoja M, Rennaker RL II, Kilgard MP. Vagus nerve stimulation during rehabilitative training improves forelimb strength following ischemic stroke. Neurobiol Dis. 2013; 60:80–88. [PubMed: 23954448]

Krahl SE, Clark KB, Smith DC, Browning RA. Locus coeruleus lesions suppress the seizure-attenuating effects of vagus nerve stimulation. Epilepsia. 1998; 39:709–714. [PubMed: 9670898]

Krahl SE, Senanayake SS, Handforth A. Destruction of Peripheral C-Fibers Does Not Alter Subsequent Vagus Nerve Stimulation-Induced Seizure Suppression in Rats. Epilepsia. 2001; 42:586–589. [PubMed: 11380564]

Linden RW. Properties of intraoral mechanoreceptors represented in the mesencephalic nucleus of the fifth nerve in the cat. J Physiol. 1978; 279:395–408. [PubMed: 671357]

Liporace J, Hucko D, Morrow R, Barolat G, Nei M, Schnur J, Sperling M. Vagal nerve stimulation: adjustments to reduce painful side effects. Neurology. 2001; 57:885–886. [PubMed: 11552021]

Manta S, Dong J, Debonnel G, Blier P. Enhancement of the function of rat serotonin and norepinephrine neurons by sustained vagus nerve stimulation. Journal of psychiatry & neuroscience: JPN. 2009a; 34:272. [PubMed: 19568478]

Manta S, Dong J, Debonnel G, Blier P. Optimization of vagus nerve stimulation parameters using the firing activity of serotonin neurons in the rat dorsal raphe. European neuropsychopharmacology. 2009b; 19:250–255. [PubMed: 19150228]

Manta S, El Mansari M, Debonnel G, Blier P. Electrophysiological and neurochemical effects of long-term vagus nerve stimulation on the rat monoaminergic systems. Int J Neuropsychopharmacol. 2013; 16:459–470. [PubMed: 22717062]

Martins ARO, Froemke RC. Coordinated forms of noradrenergic plasticity in the locus coeruleus and primary auditory cortex. Nat Neurosci. 2015; 18:1483–1492. [PubMed: 26301326]

Nichols J, Nichols A, Smirnakis S, Engineer N, Kilgard M, Atzori M. Vagus nerve stimulation modulates cortical synchrony and excitability through the activation of muscarinic receptors. Neuroscience. 2011; 189:207–214. [PubMed: 21627982]

Porter BA, Khodaparast N, Fayyaz T, Cheung RJ, Ahmed SS, Vrana WA, Rennaker RL II, Kilgard MP. Repeatedly Pairing Vagus Nerve Stimulation with a Movement Reorganizes Primary Motor Cortex. Cerebral Cortex. 2011; 22:2365–2374. [PubMed: 22079923]

Pruitt D, Schmid A, Kim L, Abe C, Trieu J, Choua C, Hays S, Kilgard M, Rennaker RL II. Vagus nerve stimulation delivered with motor training enhances recovery of function after traumatic brain injury. J Neurotrauma. 2016; 33(9):871–9. [PubMed: 26058501]

Raedt R, Clinckers R, Mollet L, Vonck K, El Tahry R, Wyckhuys T, De Herdt V, Carrette E, Wadman W, Michotte Y. Increased hippocampal noradrenaline is a biomarker for efficacy of vagus nerve stimulation in a limbic seizure model. J Neurochem. 2011; 117:461–469. [PubMed: 21323924]

Roosevelt RW, Smith DC, Clough RW, Jensen RA, Browning RA. Increased extracellular concentrations of norepinephrine in cortex and hippocampus following vagus nerve stimulation in the rat. Brain Res. 2006; 1119:124–132. [PubMed: 16962076]

Ruffoli R, Giorgi FS, Pizzanelli C, Murri L, Paparelli A, Fornai F. The chemical neuroanatomy of vagus nerve stimulation. J Chem Neuroanat. 2011; 42:288–296. [PubMed: 21167932]

Sataloff RT, Heman-Ackah YD, Hawkshaw MJ. Clinical anatomy and physiology of the voice. Otolaryngol Clin North Am. 2007; 40:909–929. [PubMed: 17765688]

Schlaepfer T, Frick C, Zobel A, Maier W, Heuser I, Bajbouj M, O'Keane V, Corcoran C, Adolfsson R, Trimble M. Vagus nerve stimulation for depression: efficacy and safety in a European study. Psychol Med. 2008; 38:651–661. [PubMed: 18177525]

Seol GH, Ziburkus J, Huang SY, Song L, Kim IT, Takamiya K, Huganir RL, Lee HK, Kirkwood A. Neuromodulators control the polarity of spike-timing-dependent synaptic plasticity. Neuron. 2007; 55:919–929. [PubMed: 17880895]

Shen H, Fuchino Y, Miyamoto D, Nomura H, Matsuki N. Vagus nerve stimulation enhances perforant path-CA3 synaptic transmission via the activation of β-adrenergic receptors and the locus coeruleus. The International Journal of Neuropsychopharmacology. 2012; 15:523–530. [PubMed: 21733240]

Shetake JA, Engineer ND, Vrana WA, Wolf JT, Kilgard MP. Pairing tone trains with vagus nerve stimulation induces temporal plasticity in auditory cortex. Exp Neurol. 2011; 233:342–49. [PubMed: 22079155]

Sokolowsky R. Effect of the extrinsic laryngeal muscles on voice production. Archives of Otolaryngology. 1943; 38:355–364.

Starke K. Presynaptic receptors. Annu Rev Pharmacol Toxicol. 1981; 21:7–30. [PubMed: 6263176]

Usami K, Kawai K, Sonoo M, Saito N. Scalp-recorded evoked potentials as a marker for afferent nerve impulse in clinical vagus nerve stimulation. Brain stimulation. 2013; 6(4):615–23. [PubMed: 23088852]

Woodbury DM, Woodbury JW. Effects of vagal stimulation on experimentally induced seizures in rats. Epilepsia. 1990; 31:S7–S19. [PubMed: 2226368]

Zuo Y, Smith DC, Jensen RA. Vagus nerve stimulation potentiates hippocampal LTP in freely-moving rats. Physiol Behav. 2007a; 90:583–589. [PubMed: 17207505]

Zuo Y, Smith DC, Jensen RA. Vagus nerve stimulation potentiates hippocampal LTP in freely-moving rats. Physiol Behav. 2007b; 90:583–589. [PubMed: 17207505]

Highlights

1. Vagus nerve stimulation drives rapid, phasic neural activity in locus coeruleus

2. Increasing current intensity and pulse width results in greater driven activity

3. Varying frequency alters the timing, but not total amount, of driven activity

4. Stronger stimulation drives off-target activity in the mesencephalic trigeminal nucleus
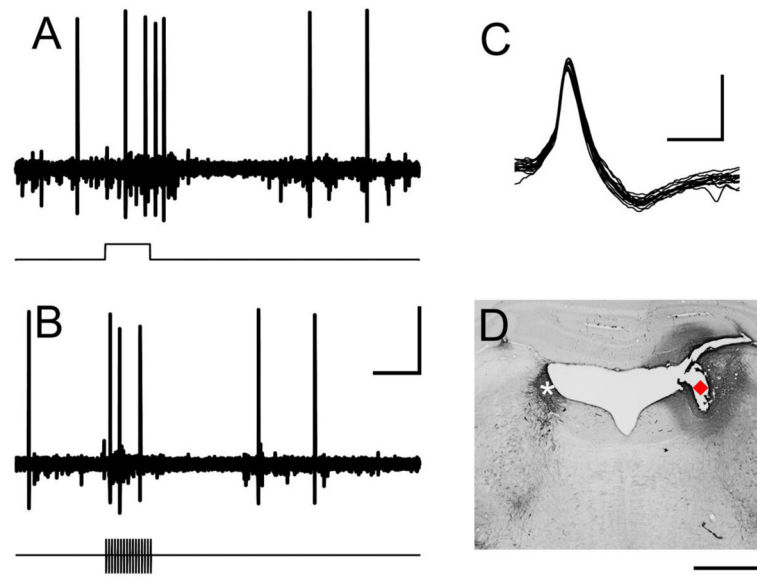
**Fig. 1. Identification of neurons in locus coeruleus**

(A) Recording sites in the LC were characterized by a brief increase in firing rate followed by a suppression in response to a hindpaw pinch (denoted by line below panel). (B) Brief trains of VNS elicited driven activity in LC neurons. (C) Characteristic wide spike shape was observed in well-isolated LC units. (D) Example histological verification of LC recording site. White * marks TH-positive neurons in LC contralateral to the recording site. Red diamond marks the electrolytic lesion location. Scale bar is 250 μV × 500 ms in panels A&B; 500 μV × 1 ms in C; 1 mm in D.
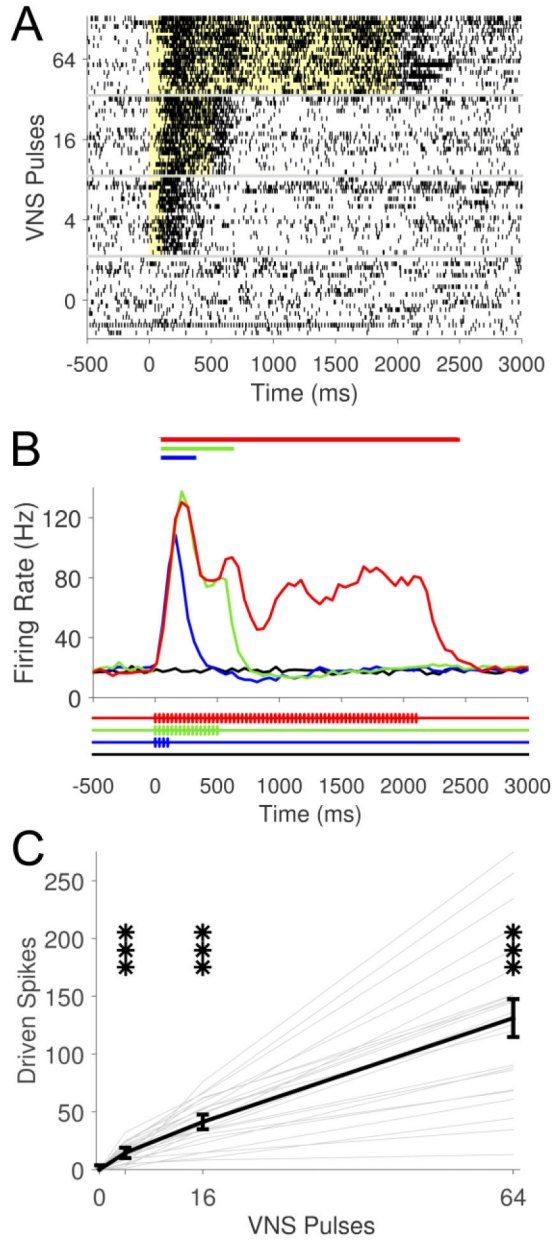
Fig. 2. VNS drives rapid, phasic neural activity in LC

(A) Example raster plot showing representative neural activity at one recording location in LC in response to 4, 16, and 64 pulse trains of VNS at 0.8 mA, 100 μs at 30 Hz. Yellow background denotes stimulation period. (B) Population PSTH of neural responses to 4 (blue), 16 (green), and 64 (red) pulses of VNS at 30 Hz. Colored lines above the PSTH represent significant positive driven response duration. VNS pulse timing is illustrated below PSTH. (C) Longer VNS train durations result in linear increases in number of driven spikes. *** p < 0.001; all statistical comparisons versus spontaneous rate.
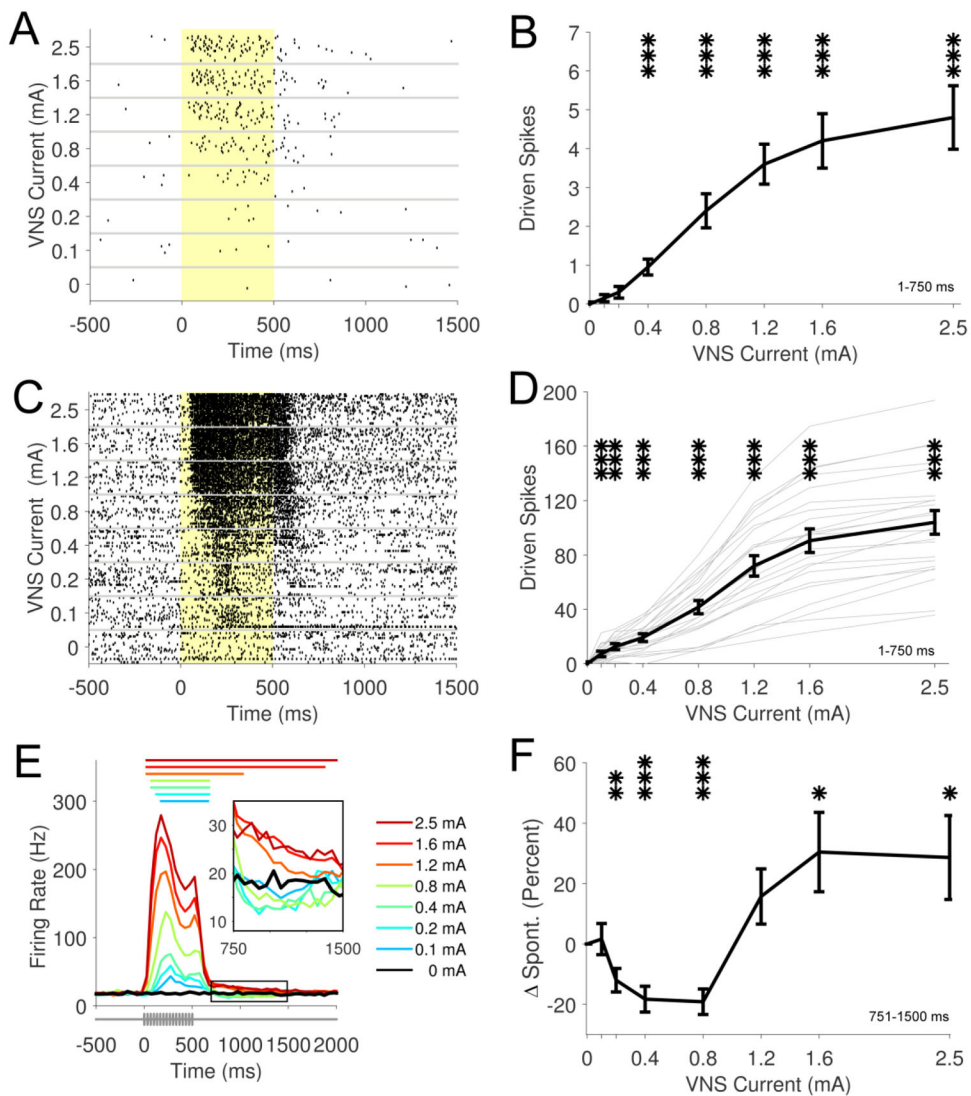
Fig. 3. Increasing stimulation intensities drive greater phasic neural activity in LC
(A) Example neural activity from a well-isolated single unit across a range of current intensities. The yellow shaded region denotes stimulation period. (B) Average driven spikes for a single unit across 20 recording sweeps between 1–750 ms response period. (C) Example multiunit recording showing phasic driven activity (1–750 ms response period) across a range of current intensities. (D) Analysis of group data of the phasic driven response (1–750 ms response period) demonstrates significant increases in driven activity at 0.1 mA stimulation intensity. Stronger current intensities drive greater increases in firing rate. Bold black line represents group average across 23 sites. Thin gray lines represent data from individual sites. (E) PSTH illustrates monotonic increases in phasic response across stimulation intensities. Colored lines above the PSTH represents significant positive driven response duration. VNS pulse timing represented below. Inset highlights offset response from 751 – 1500 ms. (F) Offset responses (751 – 1500 ms) demonstrate a modest suppression of neural activity compared to spontaneous at intensities from 0.2 – 0.8 mA and
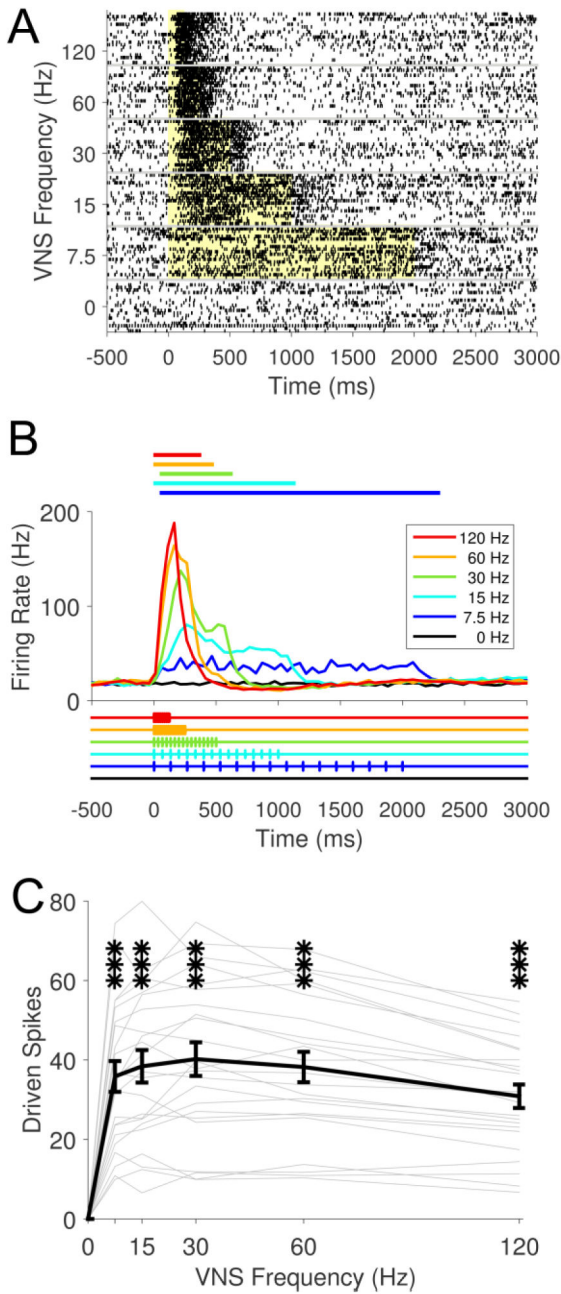
an modest increase compared to spontaneous at 1.6 mA and 2.5 mA. * p < 0.05, ** p < 0.01, *** p < 0.001; all statistical comparisons versus 0 mA (spontaneous rate).

Fig. 4. Frequency changes the timing, but not total amount of VNS-driven neural activity in LC
(A) Example raster plot from a single recording site across a range of frequencies. The yellow shaded region denotes stimulation period. (B) PSTH of population data illustrates that the timing and maximal rate of driven activity is influenced by pulse frequency. Colored lines above the PSTH represents significant positive driven response duration. VNS pulse timing represented below. Note that the number of pulses was matched across conditions. Higher frequencies drive stronger, shorter neural activity for a fixed number of pulses. (C) At all frequencies tested, VNS drives significant increases in neural activity. *** $p < 0.001$; all statistical comparisons versus 0 Hz (spontaneous rate).
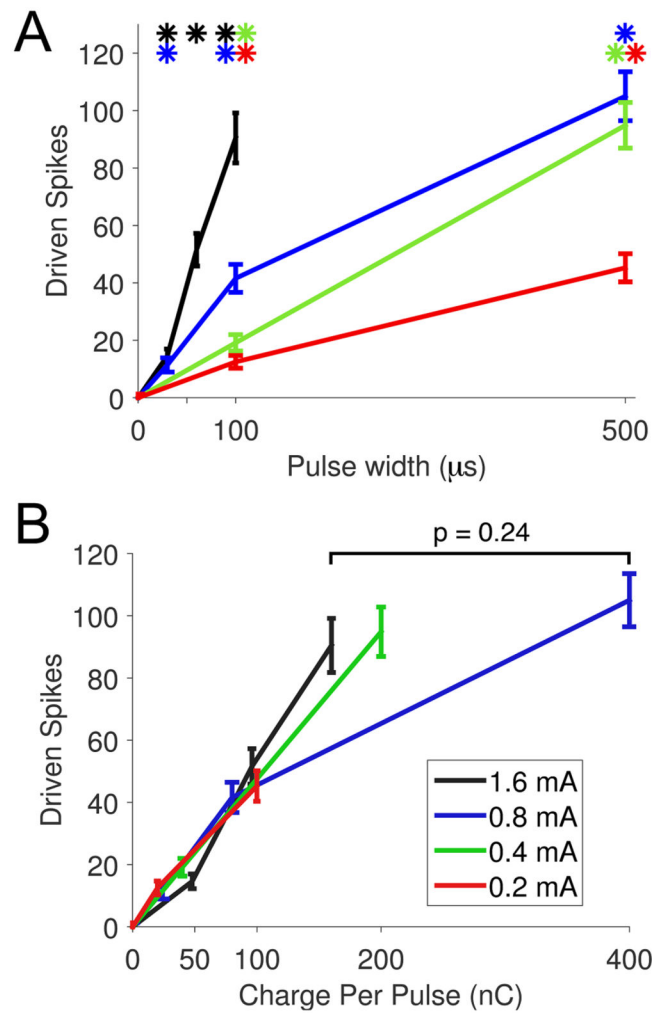
Fig. 5. Increasing pulse widths drive greater neural activity in LC
(A) At each current intensity, increasing pulse widths drive greater neural activity in LC neurons. (B) Driven spikes in the LC increase approximately linearly as a function of total charge per pulse (pulse width × current) up to 160 nC. After this point, additional charge results in diminishing increases in neural activity. Line colors in legend apply to both panels. * p < 0.001; all statistical comparisons in panel A versus 0 μs (spontaneous rate).
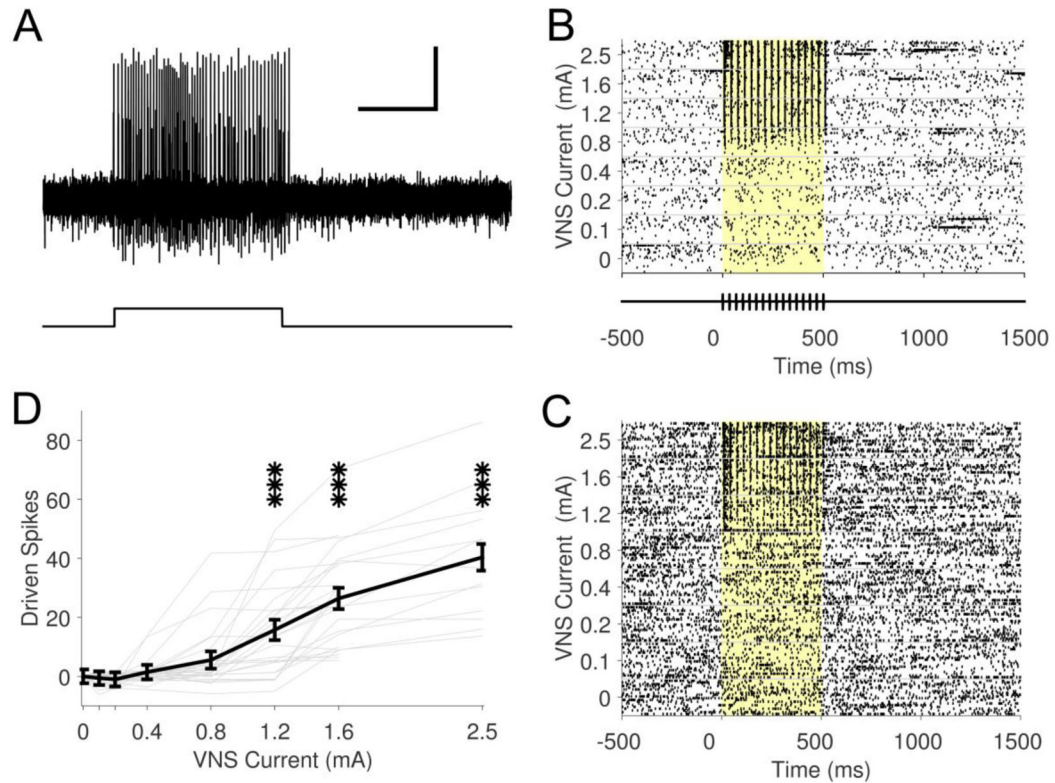
Fig. 6. VNS drives pulse-locked activity in Me5 neurons

(A) Example Me5 activity demonstrating characteristic increase in firing rate to movement of the jaw (denoted by line). (B & C) Raster plots of representative neural activity from two Me5 recording sites illustrate the strongly pulse-locked response to VNS. The yellow shaded region denotes stimulation period. Pulse timing represented below in (B). (D) Group data demonstrates a significant driven response in Me5 at 1.2 mA and above. Increasing current intensities drives stronger increases in firing rates. Bold black line represents group average across sites. Thin gray lines represent data from individual sites. *** $p < 0.001$; all statistical comparisons versus 0 mA (spontaneous rate).
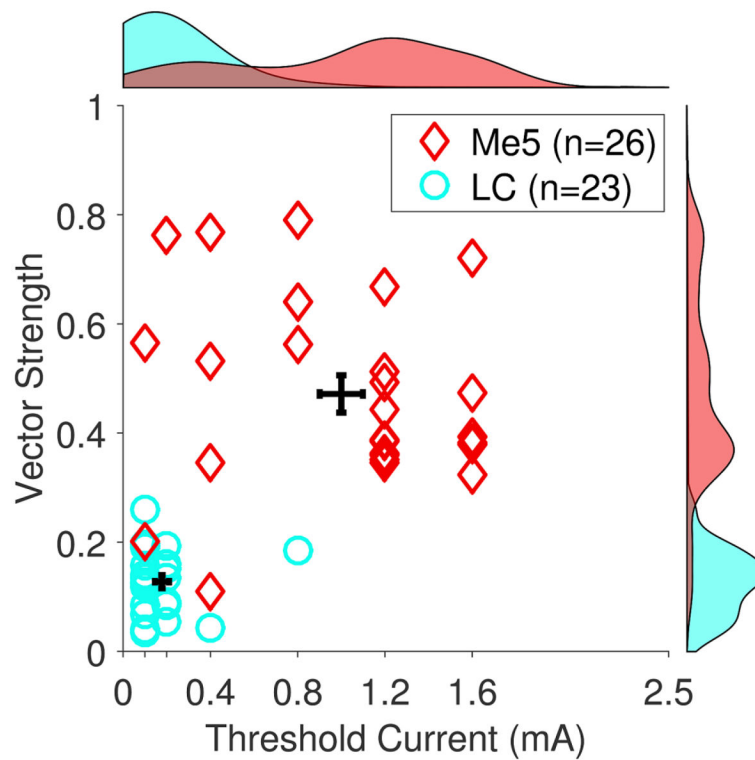
Fig. 7. Comparison of LC and Me5 response to VNS at all recording sites
Evaluation of minimum stimulation needed to evoke driven activity and degree of pulse-locking highlights distinctive LC and Me5 response to VNS. LC neurons respond at significantly lower stimulation intensities compared to Me5 neurons. Vector strength at 1.6 mA is significantly greater in Me5 neurons, representative of the strongly pulse-locked responses to individual pulses within a VNS train. Group distributions are plotted on the top and right edge.

Table 1

Range of Pulse Numbers Tested

Intensity (mA)	Pulse Width (µs)	Number of pulses	Frequency (Hz)
0	0	0	0
0.8	100	4	30
0.8	**100**	**16**	**30**
0.8	100	64	30

Standard parameters are represented in bold text

Table 2

Range of Current Intensities Tested

Intensity (mA)	Pulse Width (μs)	Number of pulses	Frequency (Hz)
0	0	0	0
0.1	100	16	30
0.2	100	16	30
0.4	100	16	30
0.8	**100**	**16**	**30**
1.2	100	16	30
1.6	100	16	30
2.5	100	16	30

Standard parameters are represented in bold text

Table 3

Range of Frequencies Tested

Intensity (mA)	Pulse Width (μs)	Number of pulses	Frequency (Hz)
0	0	0	0
0.8	100	16	7.5
0.8	100	16	15
0.8	**100**	**16**	**30**
0.8	100	16	60
0.8	100	16	120

Standard parameters are represented in bold text

Table 4

Range of Pulse Widths Tested

Intensity (mA)	Pulse Width (µs)	Number of pulses	Frequency (Hz)
0	0	0	0
0.2	100	16	30
0.2	500	16	30
0.4	100	16	30
0.4	500	16	30
0.8	30	16	30
0.8	**100**	**16**	**30**
0.8	500	16	30
1.6	30	16	30
1.6	60	16	30
1.6	100	16	30

Standard parameters are represented in bold text